



Partial Transmit Sequence and Selected Mapping Schemes for PAPR Reduction in GFDM Systems

Ari Endang Jayati^{1,2*} Wirawan Wirawan¹ Titiek Suryani¹
 Endroyono Endroyono¹

¹*Department of Electrical Engineering, Faculty of Electrical Technology,
 Institut Teknologi Sepuluh Nopember, Surabaya, Indonesia*

²*Department of Electrical Engineering, Universitas Semarang, Semarang, Indonesia*

* Corresponding author's Email: ndhank80@gmail.com

Abstract: Generalized Frequency Division Multiplexing (GFDM) is one of the 5G candidates to overcome the shortcomings of Orthogonal Frequency Division Multiplexing (OFDM), high peak rating power ratio (PAPR), and high Out of Band (OOB) radiation. GFDM has a low PAPR due to the use of a number of subcarriers. The purpose of this paper is to compare the two algorithms to reduce PAPR if applied to the non-linear distortion-affected GFDM system. Partial Transmit Sequence (PTS) and Selected Mapping (SLM) are selected because these techniques do not distort the signal, so they do not change the spectrum of the signal. The simulation result shows PAPR GFDM is not significantly affected by nonlinear distortion. After being given the PTS technique, the PAPR value on GFDM dropped to 5 dB. Meanwhile, after being given a selective mapping technique, the PAPR value in GFDM dropped to 6.2 dB.. However, for a 5G application with thousands of devices, this value should still be reduced. After being given a PTS, the PAPR value drops to the value according to the 5G criterion. Better PTS performance decreases PAPR for GFDM systems that are given nonlinear distortion when compared to SLM.

Keywords: GFDM, PAPR, PTS, SLM, 5G.

1. Introduction

Generalized Frequency Division Multiplexing (GFDM) is one of the 5G candidates to overcome the shortcomings of OFDM that has high PAPR values and high OOB radiation. GFDM has a low PAPR due to the use of a number of subcarriers [1] and low Out-of-Band (OOB) radiation. This is because it uses pulse shaping of the raised cosine type and uses only one CP on a set of GFDM symbol groups to produce more efficient bandwidth [2].

Just like other multicarrier systems, GFDM also uses High Power Amplifier (HPA) in the transmitter side. The use of HPA in the transmitter is necessary in order for the signal to be transmitted properly, but setting the HPA closer to its saturation point increases power efficiency and adjusts the HPA above the linear region resulting in a nonlinear distortion effect

[3]. Nonlinear distortion causes some effects such as generating new signal components with three times the frequency of the basic components in the third-order nonlinearity [4]. The nonlinear distortion also raises the signal spectrum sidelobe which will result in interference between adjacent subcarriers [5]. It can also cause deformation and dispersion of signal constellations as well as amplitude and phase distortion [6].

There is a trade-off between computational complexity, PAPR reduction capability, and BER performance. Like other multicarrier systems, GFDM suffers from a high average peak power ratio (PAPR). The GFDM feature can solve this problem by reducing the number of subcarriers and changing the pulse shaping filter parameters. However, in any multicarrier system, reducing the number of subcarriers always leads to PAPR reduction and does not solve the problem. As a result, there is still a need

to reduce the peak value to the lowest level when having many subcarriers [7]. Michailow et al have compared PAPR between GFDM and OFDM for unequal number of subcarriers [8]. Precoding can be used to improve SER system performance through selective frequency channels and to reduce PAPR. The best PAPR decrease was achieved by the CAZAC transformation, followed by DHT and WHT [9]. The effect of the pulse shaping filter on the PAPR performance of the GFDM system has been investigated and the PAPR comparison on OFDM and GFDM is also shown. The selection of pulse-forming filters has a major influence on the performance of GFDM communication systems. Thus, PAPR is influenced by same filter factor as different roll-off factors or different filters with the same roll-off factor [10].

PTS and selected mapping techniques are used to reduce the increase in PAPR due to the application of high power amplifiers. PTS techniques are known for achieving high performance and redundancy utilization. Both of these techniques are indeed not new techniques. To our knowledge, there is no application of this technique in orthogonal waves, namely GFDM. GFDM is one of the orthogonal wave candidates for future generation networks. Because the subcarrier in GFDM is a pulse shaping, it experiences high signal envelope fluctuations, so the nonlinear characteristics of the high power amplifier (HPA) cause a large decrease in performance.

Several PAPR reduction techniques, to overcome nonlinear problems, have been introduced in the literature. Research to reduce PAPR on GFDM has been carried out, namely the iterative receiver clipped GFDM method. The results show that GFDM in special cases can outperform OFDM. To our knowledge, there is no research on the application of these techniques to overcome nonlinear distortion in GFDM systems. Therefore, in this paper, we investigate the application of PTS techniques and selective mapping to GFDM systems by HPA and analyze the performance of PAPR.

This paper has the following sections: The next section discusses about how the system model GFDM is given nonlinear distortion. Section III discusses the review of SLM and PTS methods. In section IV we discuss simulation results with PAPR parameter to compare both methods on OFDM system.

2. Literature review

Techniques for mitigating nonlinear distortion in addition to PAPR reduction techniques can also use HPA linearization techniques. Other PAPR reduction

techniques such as Clipping and Tone Reservation have also been studied by [12]. The weakness of this research is that it increases complexity in the transmitter.

Muller et al. proposed a highly effective and flexible peak power reduction scheme for OFDM. This method combines partial transmit sequences (PTS) to minimize peak-to-average power ratios without distortion [13]. The drawback of this research is that this technique has additional redundancy and adds complexity to the transmitter.

Kumar et al. has carried out research on PTS enhanced by the new Block Weighting (SW) method. Enhanced PTS is combined with SLM techniques to reduce computing complexity for OFDM systems [14]. The advantage of this work is that this technique combines with selective mapping to reduce computational complexity. The drawback is that the resulting CCDF and BER are still rough, the number of symbols processed is not much.

Maddala et al. proposed another PTS scheme that had been industrialized to reject the PAPR. This method selects the ideal stage factor price through a flexible ABC optimization process. At the point when applied to MIMO-OFDM systems with various phase factors, this method can reduce the complexity of computing for larger PTS subblocks and offer lower PAPR [15]. The weakness of Maddala's research is that this technique is applied in the orthogonal MIMO OFDM system which is not yet in the non-orthogonal waveform system.

Research on the effects of nonlinear distortion on Multiple Input Multiple Output (MIMO)-GFDM systems when signals are passed by HPA has been carried out by [16]. In addition, they also propose methods to overcome these problems. The proposed method is the application of a predistorter technique for linearization of each HPA on the transmitter side of the MIMO-GFDM system separately. This predistorter is able to compensate for nonlinear distortion caused by memoryless HPA that operates in the saturation region.

In this paper we propose Selected Mapping and Partial Transmit Sequence reducing PAPR on nonlinear distorted GFDM systems. Selected Mapping was first introduced in [11]. Meanwhile, the second algorithm, PTS, was introduced by [12]. The purpose of this paper is to compare the PAPR parameters of both algorithms.

3. Proposed systems

3.1 System model

We use the GFDM scheme shown in figure 1. The binary data row \vec{b} generated by the data source is encoded into \vec{b}_c . The data are mapped to a row of symbols in the mapper block using 16-OQAM modulation to produce vector data \vec{d} . The vector is then converted to low speed rate data and decomposed into GFDM blocks of $K \times M$ size in the GFDM modulator block, where K and M respectively denote the number of subcarrier and subsymbol samples for each GFDM block. Therefore, the decomposition vector is $\vec{d} = d_{0,0}, d_{1,0}, \dots, d_{K-1,M-1}$. Data vectors \vec{d} is split into two, real value data d_i and imaginary data d_q . Then the data are filtered by pulse shaping using Root Raised Cosine with the following equation [17]:

$$g_{k,m}(n) = g \left[\left(n - \frac{mK}{2} \right) \bmod KM \right] e^{\frac{j2\pi k}{K} \left(n - \frac{Lp-1}{2} \right)} \quad (1)$$

Where: $n = 0.1, \dots, KM-1$

Lp = the length of the filter prototype

Pulse shaping of each subcarrier and subsymbol is grouped into a modulation matrix as follows:

$$A = [g_{0,0} \dots g_{K-1,0} \dots g_{0,1} \dots g_{K-1,M-1}] \quad (2)$$

The OQAM process will transmit the real part of the QAM symbol data using pulse shaping and the quadrature with a shift of $K / 2$ samples or half subcarriers to each other. So the pulse shaping can be written as follows [18]:

$$\begin{aligned} g_{k,m}^{(i)}[n] &= j^k g_{k,m}[n] \\ g_{k,m}^{(q)}[n] &= j^{k+1} g_{k,m+\frac{1}{2}}[n] \end{aligned} \quad (3)$$

The output of the modulator can be represented as follows:

$$x(n) = \sum_{m=0}^{M-1} \sum_{k=0}^{K-1} d_{k,m}^{(i)} g_{k,m}^{(i)}[n] + \sum_{m=0}^{M-1} \sum_{k=0}^{K-1} d_{k,m}^{(q)} g_{k,m}^{(q)}[n] \quad (4)$$

And can also be written in matrix form [19]:

$$x = A^{(i)} d^{(i)} + A^{(q)} d^{(q)} \quad (5)$$

The output of the modulator can also be written in the form of baseband [17]:

$$x(n) = \sum_{k=0}^{K-1} \sum_{m=0}^{M-1} a_k(m) g_{k,m}(n) e^{j\phi_{m,k}} \quad (6)$$

Where: $n = 0.1, \dots, KM-1$, $a_k(m)$ = complex data obtained from the complex part of the QAM constellation, $\phi_{m,k} = \frac{(k+m)\pi}{2}$ = phase difference $\pi / 2$ time domain

Then the PAPR modulator output are reduced using PTS or SLM. The output from the PTS block is then added to CP and given a nonlinear distortion of Saleh Model where the output signal from High Power Amplifier (HPA) can be modeled:

$$z[n] = g(r(n)) e^{j(\theta+f(r(n)))} \quad (7)$$

With $g(r(n))$ is the AM/AM conversion function of the signal amplitude and $f(r(n))$ is the AM/PM conversion function of the phase signal.

$$\begin{aligned} g(r(n)) &= \frac{\alpha_\alpha r(n)}{[1+\beta_\alpha]r(n)^2} \\ f(r(n)) &= \frac{\alpha_\phi r(n)^2}{[1+\beta_\phi]r(n)^2} \end{aligned} \quad (8)$$

Where $\alpha_\alpha, \beta_\alpha, \alpha_\phi, \beta_\phi$ are Saleh model parameters [20].

After the signal is given a nonlinear distortion then the signal is transmitted through the channel and given the AWGN noise so the equation becomes [4]:

$$\vec{y} = F_{NL}[\vec{Xp}] + \vec{n} \quad (9)$$

With $F_{NL}[\cdot]$ representing nonlinear function of HPA. $[\vec{Xp}]$ represents the output signal of the PAPR reduction technique and \vec{n} is the Additive White Gaussian Noise notation (AWGN) $\vec{n} \sim N(0, \sigma_n^2 I_{MN})$ with the variance noise σ_n^2 and I_{MN} is a sized identity matrix $MN \times MN$.

The next process is to pass the equalizer after the removal of CP at the receiver side. Zero Forcing Receiver as follows [21]:

$$\hat{a}_{ZF} = A^+ \vec{y} \quad (10)$$

Where A^+ can be computed with $A^+ = (A^H A)^{-1} A^H$.

Then after equalizer is demodulation process of GFDM by converting it to the frequency domain, precisely by multiplying the transpose form from matrix A_i and A_q result IFFT with the signal transmitted after CP reduction [21].

$$d = \Re \{ (\tilde{A}^{(i)})^H y \} + j \Re \{ \tilde{A}^{(q)}{}^H y \} \quad (11)$$

Where: $\tilde{A}^{(i)} = W_N^H A^{(i)}$ and $\tilde{A}^{(q)} = W_N^H A^{(q)}$ with W_N is the DFT matrix $[W_N]_{i,l} = \frac{\exp(-j2\pi \frac{il}{N})}{\sqrt{N}}$.

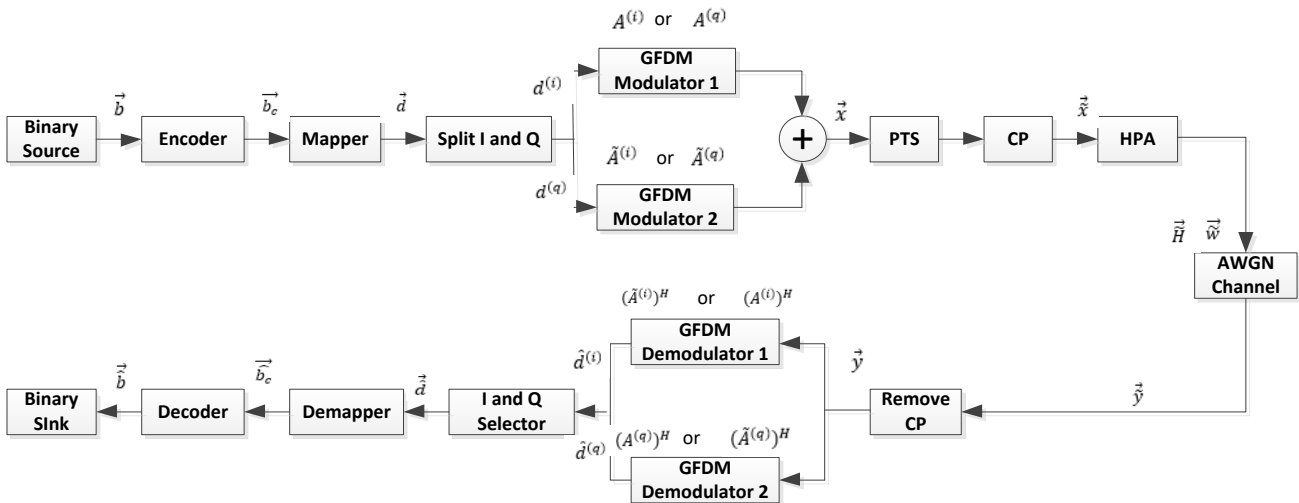


Figure 1. Block diagram of PTS on GFDM

The above results are still parallel and then serialized for demodulation process in the next stage using Parallel to Serial converter at receiver. Then the GFDM symbol is converted into bits again.

3.2 Partial transmit sequence and selected mapping

The efficiency of HPA power increases if the HPA is working near or within the saturation region where the amplitude of the HPA input is close to the saturation value of A_{sat} , e.g. $A_{max} \approx A_{sat}$, the input signal with $A_{max} / 2 \sim A_{max}$ amplitudes, which can not be compensated, which causes the PSD to rise and decrease in performance. PAPR reduction techniques are used to overcome them [19].

The PAPR reduction technique reduces the envelope fluctuation of the signal transmitted by the PA. The easiest way to reduce PAPR is to bypass the signal on the transmitter. Cutting operation distorts the original signal and raises OOB and BER. Some approaches to reducing PAPR without signal distortion are called distortionless techniques such as PTS, TR, TI, and SLM [22].

There are 2 types of PAPR reduction techniques, deterministic and probabilistic. Probabilistic categories, such as PTS and SLM, statistically increase the PAPR distribution of the signal by avoiding signal distortion. PTS and SLM are multiplication types because their sequence are multiplied by the signal vector. All techniques reduce PAPR but can increase complexity, high BER, transmission power, and data rate loss. Therefore, the technique used is one that minimizes PAPR and can

improve performance as needed. PAPR studied in this research are PTS and SLM. PTS and SLM are chosen because these techniques do not distort the signal, so they do not change the spectrum of the signal [22].

In this paper, we consider PAPR reduction technologies of PTS and SLM to compare PAPR through nonlinear channels. This scheme for uplink system uses GFDM that meets the 5G requirements. In the next section we discuss various techniques used to reduce PAPR, i.e. PTS and SLM.

3.2.1. Partial transmit sequence

PTS is one of the randomization techniques to reduce PAPR. The basic idea of this technique is to form a combined weight of the disjoint subblock, then select the one that has the smallest PAPR value to transmit. The block diagram of PTS can be seen in figure 2 which can be explained by the following steps [23]:

The Output sequence of the modulator, X , is partitioned into a V disjoint subblock. Each subblock has the same size:

$$X_v = \{X_v^0, X_v^1, \dots, X_v^{N-1}\}, v = 0, 1, \dots, V - 1 \quad (12)$$

Apply a number of LN IFFT points to each XV to get the xv subblocks in the time domain represented as follows:

$$x_v = IFFT\{X_v\} \quad (13)$$

Each time domain subblock is multiplied by the corresponding complex weighting factor, which can be written as follows:

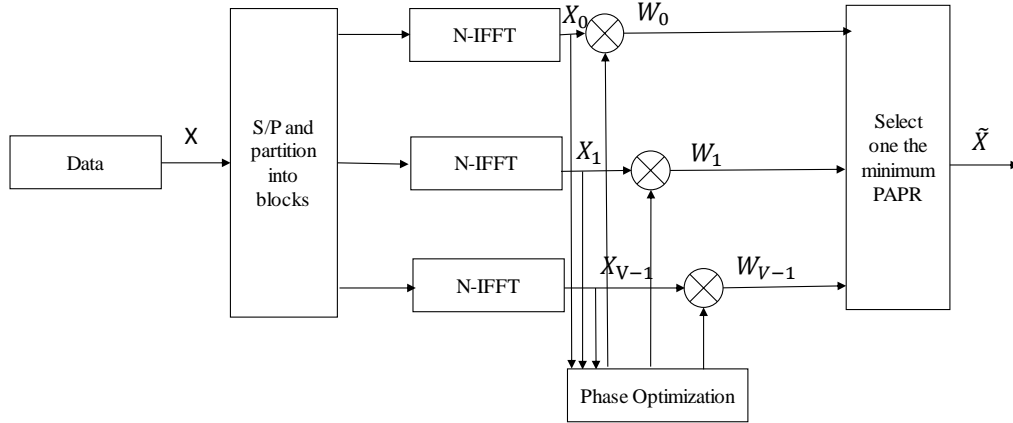


Figure 2. Block diagram PTS

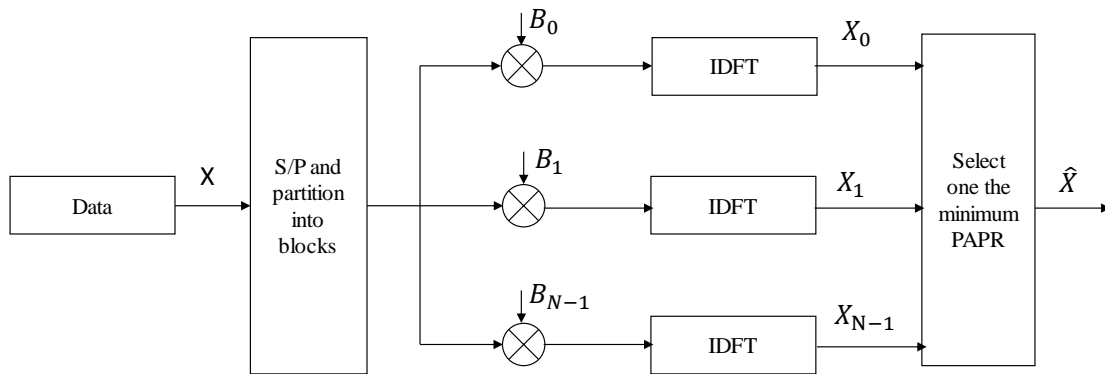


Figure 3. Block diagram of SLM

$$x = \sum_{v=0}^{V-1} w_v x_v \tag{14}$$

$$X = [X_0, X_1, X_2, \dots, X_{N-1}]^T \tag{17}$$

Where: $w_v = e^{j\theta v}$ is a phase factor with $v = 0, 1, \dots, v-1$.

Choose a suitable rotation factor to make the minimum PAPR as follows:

$$\tilde{w}_v = \underset{w_v}{\operatorname{argmin}} \left(\max_{0 < n < LN-1} \left| \sum_{v=0}^{V-1} w_v x_v \right| \right) \tag{15}$$

Where: $\tilde{w}_v = \{\tilde{w}_0, \tilde{w}_1, \dots, \tilde{w}_{v-1}\}$ is the optimum rotation factor.

The optimized transmission signal becomes:

$$\tilde{x} = \sum_{v=0}^{V-1} \tilde{w}_v x^{(v)} \tag{16}$$

3.2.2. Selected mapping

Selected Mapping (SLM) reduces the probability of a high peak but does not eliminate the peak. Bauml et al. (1996) proposed this method whereby the SLM scheme was introduced as one of the initial probabilistic approaches and compatible with a number of subcarriers. In this method, the input data are divided into several sub-blocks and converted to parallel by the converter. The input data are defined as [8]:

Then the input data sequence is multiplied by the phase sequence to generate the sequence of input symbols. The phase sequence is rotated by rotation factor Bv^u .

$$X^{vu} = \text{IFFT}(X \otimes B^{(vu)}) \tag{18}$$

Where $B^u = [bv_0^u, bv_1^u, bv_2^u, \dots, bv_{N-1}^u]^T$ In the order of phases: $|bv_n^u| = 1, (n = 0, 1, N - 1)$.

± 1 is usually chosen to avoid complexity of complex multiplication or to add unmodified data to modified data. After that multiply the input data with phase difference U. The order of phase U is $X^u = [X_0 bv_{u,0}, X_1 bv_{u,1}, X_2 bv_{u,2}, \dots, X_{N-1}, bv_{u,N-1}]$. Where $u = 0, 1, 2, \dots, U - 1$.

After the comparison between the U data sequences x (u), the most optimally mapped one x with the minimum PAPR is selected:

$$\hat{x} = \operatorname{arg min}_{0 \leq u \leq U} [PAPR(X^{(vu)})] \tag{19}$$

The steps of PTS on the GFDM system are summarized in the following algorithm-1. Furthermore, the SLM steps in the GFDM system are written in the following algorithm-2.

Algorithm-1 Modelling of PTS for GFDM systems		
1:	$\mathbf{d} \leftarrow \mathbf{b}$	▷ mapping 16 OQAM
2:	$\mathbf{A} \leftarrow \mathbf{g}$	▷ pulse shaping RRC
3:	$\mathbf{x} \leftarrow \mathbf{A}\mathbf{d}$	▷ output GFDM
4:	$\mathbf{X}\mathbf{v} \leftarrow \mathbf{X}$	▷ partition into subblock
5:	$\mathbf{x}\mathbf{v} \leftarrow \mathbf{X}\mathbf{v}$	▷ IFFT
6:	For $\mathbf{v}=0:\mathbf{V}-1$	
7:	$\mathbf{X}=\mathbf{w}\mathbf{v}\mathbf{x}\mathbf{v}$	▷ multiplied with weighting factor
8:	$\tilde{\mathbf{w}}_v \leftarrow \mathbf{X}$	▷ choose minimum PAPR
9:	$\tilde{\mathbf{x}} \leftarrow \tilde{\mathbf{w}}_v \cdot \mathbf{x}$	▷ optimized signal
10:	end for	

Algorithm-2 Modelling of SLM for GFDM systems		
1:	$\mathbf{d} \leftarrow \mathbf{b}$	▷ mapping 16 OQAM
2:	$\mathbf{A} \leftarrow \mathbf{g}$	▷ pulse shaping RRC
3:	$\mathbf{x} \leftarrow \mathbf{A}\mathbf{d}$	▷ output GFDM
4:	$\mathbf{X} \leftarrow \mathbf{X}_N$	▷ partition into subblock
5:	For $\mathbf{n}=0:\mathbf{N}-1$	
5:	$\mathbf{x}^{\mathbf{v}\mathbf{u}} \leftarrow \mathbf{X} \otimes \mathbf{B}(\mathbf{v}\mathbf{u})$	▷ multiplied with rotation factor
6:	$\mathbf{X}^{\mathbf{v}\mathbf{u}} \leftarrow \mathbf{x}^{\mathbf{v}\mathbf{u}}$	▷ IFFT
8:	$\mathbf{PAPR}(\mathbf{X}^{\mathbf{v}\mathbf{u}})$	▷ choose minimum PAPR
9:	$\tilde{\mathbf{x}} \leftarrow \mathbf{PAPR}(\mathbf{X}^{\mathbf{v}\mathbf{u}})$	▷ optimized signal
12:	end for	

4. Result and discussion

Results are obtained through Matlab simulation. Figure 4 shows a CCDF graph between GFDM and OFDM if given a PTS reduction technique with simulation parameters such as Table 1. The parameter for PTS is the number of symbols: 100, the number of subband: 64, the oversampling factor: 4, the possible phase factor (p) value: 4, phase factor permutation (B): 256 x 4 of (64 x 4). It is seen that PAPR for GFDM when compared OFDM before being given the PTS reduction technique in CCDF 0.01 PAPR GFDM value is about 8.8 dB whereas OFDM is about 8.6 dB. This is because each subcarrier on GFDM has a circular signal property in time and frequency domain [4]. After being given a PTS technique, the PAPR value drops to below 5 dB.

The next graph is if GFDM is given linear distortion with Saleh Model as shown in figure 5. Parameter Model Saleh: $\alpha_\alpha = 2.1587$; $\beta_\alpha = 1.1517$; $\alpha_\phi = 4.033$; $\beta_\phi = 9.1040$. Modeling of nonlinear distortion was mentioned in the previous section, namely in equation 8. With the Saleh Model parameter values taken from experimental data conducted by Saleh in 1981[20]. There are 2

representation functions, namely $g(r(n))$ as a function of AM / AM conversion of the signal amplitude, and $f(r(n))$ as a function of AM / PM conversion of the signal phase.

Visible PAPR GFDM is not affected by nonlinear distortion, but still around the value of 9 dB and above. For a 5G application with thousands of devices, this value should still be reduced. After being given a PTS, the PAPR value drops to a value below 5 dB.

The next PAPR reduction technique is SLM, as shown in figure 6 with the simulation parameters in Table 2 with SLM parameters, number of symbols, i.e.: 100, Subband count: 64, oversampling factor: 4, number of candidate symbols GFDM (C): 16, permutations Factor Phase (B): 16 x 64. Figure 7 shows that the PAPR for GFDM compared to OFDM before the SLM reduction technique in CCDF 0.01 PAPR GFDM value is about 8.8 dB whereas OFDM is about 8.6 dB. After being given a PTS technique, the PAPR GFDM value drops to below 6.2 dB, whereas OFDM drops to 6.8 dB. After being given the PTS technique, the GFDM PAPR decreased significantly. However, PTS performance is better when compared to SLM techniques. Then if given Saleh Model for nonlinear distortion as in Figure 8, it is seen that PAPR GFDM is not affected by nonlinear distortion, but still around 9 dB and above. After being given a SLM, the PAPR value drops to 6.2 dB.

This study only compares PAPR between PTS and SLM techniques in GFDM if given nonlinear distortion. PTS and SLM do not change the GFDM spectrum because these techniques do not increase the OOB noise floor [4]. BER performance in the GFDM system if given a nonlinear distortion is strongly related to the type of filter and its parameters [21].

Table 1. Parameter PTS OFDM vs GFDM

Parameter	OFDM	GFDM
Number of Sub carriers	64	64
Modulation type	QPSK	QAM
Number of Symbols	1000	1000
Pulse Shaping	rectangular	Raised cosine
Roll-off factor		0.5
Number of Symbol Candidates for Phase Factor Matrix (B)	16	16
Phase factor combination	$\pm 1, \pm j$	$\pm 1, \pm j$
Oversampling factor	4	4

Table 2. Parameter SLM OFDM vs. GFDM

Parameter	OFDM	GFDM
Number of Sub carriers	64	64
Modulation type	QPSK	QAM
Number of Symbols	1000	1000
Number of Sub Blocks	4	4
Phase factor combination	$\pm 1, \pm j$	$\pm 1, \pm j$
Oversampling factor	4	4

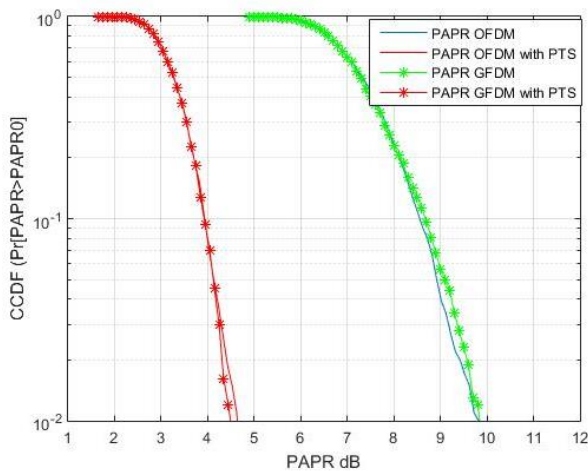


Figure 4. Comparison of PTS on GFDM and OFDM

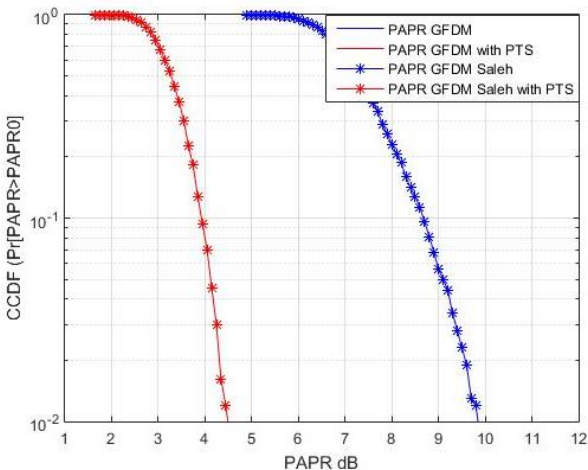


Figure 5. PAPR PTS on GFDM with Nonlinear Distortion

The PAPR reduction technique is only one way to overcome nonlinear distortion due to HPA. In the next study, other techniques are investigated to overcome nonlinear distortion in the MIMO-GFDM system. These other techniques will also be investigated by the effect of coding on the performance of the system.

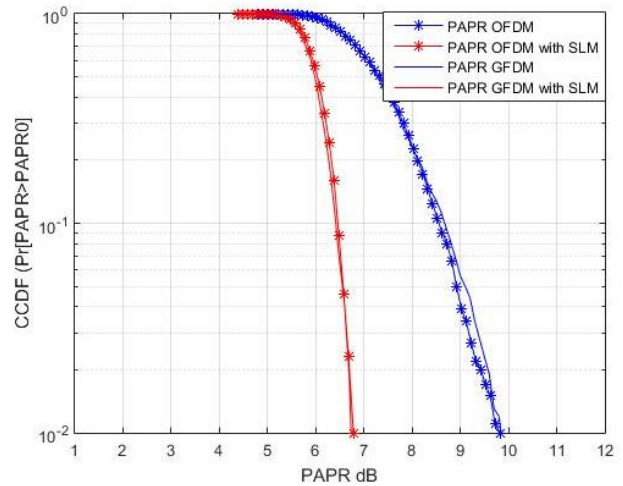


Figure 6. Comparison of SLM on GFDM and OFDM

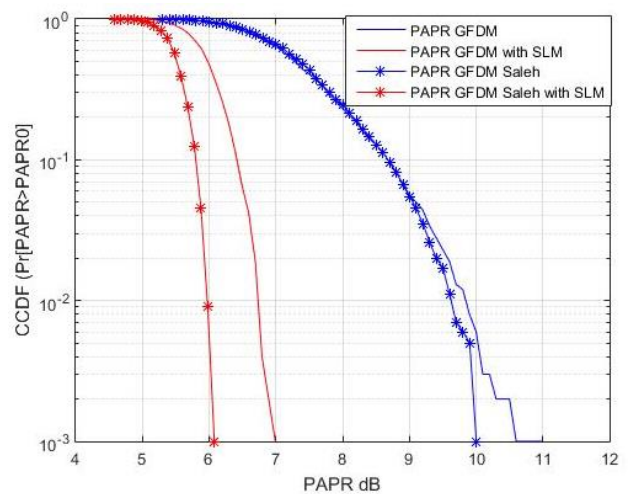


Figure 7. PAPR SLM on GFDM with Nonlinear Distortion

5. Conclusion

In this paper we have compared two PAPR reduction techniques, namely Selected Mapping and Partial Transmit Sequence, to reduce PAPR if applied to GFDM systems affected by nonlinear distortion. Visible PAPR GFDM is not affected by nonlinear distortion. For a 5G application with thousands of devices, this value should still be reduced. After being given the PTS technique, the PAPR value on GFDM dropped to 5 dB. Meanwhile, after being given a selective mapping technique, the PAPR value in GFDM dropped to 6.2 dB. So the PTS technical performance is better than selective mapping. After being given a PTS, the PAPR value drops to the value according to the 5G criterion. Better PTS performance decreases PAPR but when compared to SLM for GFDM given nonlinear distortion. Future research is needed to apply this technique to overcome nonlinear distortions in the MIMO-GFDM system.

Acknowledgments

This work was supported by Semarang University.

References

- [1] N. Michailow and G. Fettweis, "Low Peak-to-Average Power Ratio for Next Generation Cellular Systems with Generalized Frequency Division Multiplexing," In: *Proc. of 2013 IEEE International Symposium on Intelligent Signal Processing and Communication Systems*, pp. 651–655, 2013.
- [2] N. Michailow, R. Datta, S. Krone, M. Lentmaier, and G. Fettweis, "Generalized Frequency Division Multiplexing: A Flexible Multi-Carrier Modulation Scheme for 5th Generation Cellular Networks," In: *Proc. of Ger. Microw. Conf.*, Vol. 62, No. 9, pp. 1–4, 2014.
- [3] K.M. Gharaibeh, "Non Linear Distortion in Wireless Communication Using Matlab", Wiley, 2012.
- [4] A. Ortega and L. Fabbri, "Performance evaluation of GFDM over nonlinear channel", In: *Proc. of ICTC 2016*, pp. 12–17, 2016.
- [5] P. Jantunen, "Modelling of Nonlinear Power Amplifiers for Wireless Communications", Thesis, Finland, 2004.
- [6] A. E. Jayati, Wirawan, and T. Suryani, "Analysis of Non-Linear Distortion Effect Based on Saleh Model in GFDM System", In: *Proc. of IEEE International Conference on Commnetsat*, pp. 13–18, 2017.
- [7] Z. Sharifian, M.J Omid, A. Farhang, H. Saeedi-Sourck, "Polynomial-based compressing and iterative expanding for PAPR reduction in GFDM", In: *Proc of the 23rd Iran Conf. Electr. Eng.*, pp. 518-523, 2015.
- [8] H. Tiwari, R. Roshan, and R. K. Singh, "PAPR Reduction in MIMO-OFDM using Combined Methodology of Selected Mapping (SLM) and Partial Transmit Sequence (PTS)", In: *Proc. of International Conference on Industrial and Information Systems (ICIIS)*, No. 1, pp. 1-5, 2014.
- [9] M. Matthé, D. Zhang, and G. Fettweis, "Iterative Detection using MMSE-PIC Demapping for MIMO-GFDM Systems", In: *Proc. of IEEE European Wireless (EW '16)*, pp. 473–479, 2016.
- [10] J. Wu, X. Ma, X. Qi, Z. Babar, W. Zheng, "Influence of pulse shaping filters on PAPR performance of underwater 5G communication system technique", *Wirel. Commun. Mob. Comput.*, 2017.
- [11] R. Bauml, R. Fischer, and J. Huber, "Reducing the Peak-to-Average Power Ratio of Multicarrier Modulation by Selected Mapping", *Electron. Lett.*, Vol. 32, No. 22, pp. 2056-2057, 1996.
- [12] H. Abdelali, S. Bachir, and M. Oumsis, "New Technique Combining the Tone Reservation Method with Clipping Technique to Reduce the Peak-to-Average Power Ratio", *International Journal of Electrical and Computer Engineering*, Vol. 8, No. 6, pp. 5215–5226, 2018.
- [13] S. H. Müller and J.B Huber, "OFDM with reduced peak-to-average power ratio by optimum combination of partial transmit sequences", *Electron Letter*, 1997.
- [14] K. K. Kumar, "Improved PTS Technique Based on Sub-Block Weighting Method of PAPR Reduction in OFDM Signals", *International Journal of Intelligent Engineering and Systems*, Vol. 10, No. 5, pp. 87–94, 2017.
- [15] V. Maddala and R.R Katta, "Adaptive ABC Algorithm Based PTS Scheme for PAPR Reduction in MIMO", *International Journal of Intelligent Engineering and Systems*, Vol. 10, No. 2, pp. 48–57, 2017.
- [16] A. E. Jayati, Wirawan, T. Suryani, and Endroyono, "Nonlinear Distortion Cancellation using Predistorter in MIMO-GFDM Systems", *Electronics*, Vol. 8, No. 620, pp. 1-19, 2019.
- [17] S. K. Bandari and V. V. Mani, "OQAM implementation of GFDM", In: *Proc. of ICT*, pp. 1-5, 2016.
- [18] I. S. Gaspar, "Waveform Advancements and Synchronization Techniques for Generalized Frequency Division Multiplexing Waveform", *Ph.D. Thesis*, Technische Universitat Dresden, 2016.
- [19] A. Bo, Y. Zhi-xing, P. Chang-yong, Z. Tao-tao, and G. Jian-hua, "Effects of PAPR Reduction on HPA Predistortion", *IEEE Trans. Consum. Electron.*, Vol. 2, No. 4, pp. 1143–1147, 2005.
- [20] A. A. Saleh, "Frequency-Independent and Frequency-Dependent Nonlinear Models of TWT Amplifiers", *IEEE Trans. Commun.*, No. 29, pp. 1715–1720, 1981.
- [21] L. Sendrei, S. Marchevsky, M. Lentmaier, and G. Fettweis, "Iterative receiver for clipped GFDM signals", In: *Proc. of the 24th Intl. Conference Radioelektronika (RADIOELEKTRONIKA)*, No. 1, pp. 14-17, 2014.
- [22] F. H. Gregorio, "Analysis and Compensation of Nonlinear Power Amplifier Effects in Multi-antenna OFDM Systems", *Dissertation*, Helsinki University of Technology, 2007.
- [23] C. B. A. Wael, N. Armi, and P. A. R. Budiman, "PTS-Based PAPR Reduction in Fixed WiMAX System With Grouping Phase Weighting

(GPW)", In: *Proc. of IEEE International Conf. on Telecommunication Systems, Services, and Applications (TSSA)*, pp. 1-5, Nov. 2015.